European Journal of Nuclear Medicine and Molecular Imaging (2021) 48:4508–4516
https://doi.org/10.1007/s00259-021-05426-9

ORIGINAL ARTICLE

^{64}Cu-PSMA-BCH: a new radiotracer for delayed PET imaging of prostate cancer

Teli Liu[1] · Chen Liu[1] · Zhongyi Zhang[2] · Ning Zhang[3] · Xiaoyi Guo[1] · Lei Xia[1] · Jinquan Jiang[1] · Qing Xie[1] · Kun Yan[2] · Steven P. Rowe[4] · Hua Zhu[1] · Zhi Yang[1]

Received: 17 February 2021 / Accepted: 24 May 2021 / Published online: 25 June 2021

Abstract

Purpose Develop a ^{64}Cu labeled radiopharmaceutical targeting prostate specific membrane antigen (PSMA) and investigate its application for prostate cancer imaging.

Methods ^{64}Cu-PSMA-BCH was prepared and investigated for stability, PSMA specificity, and micro-PET imaging. With the approval of Ethics Committee of Beijing Cancer Hospital (No. 2017KT97), PET/CT imaging in 4 patients with suspected prostate cancer was performed and the radiation dosimetry was estimated. Then, PSMA PET-ultrasound image-guided biopsies were performed on 3 patients and the fine needle aspirates were further performed for autoradiography and immunohistochemistry analysis.

Results ^{64}Cu-PSMA-BCH was prepared with high radiochemical yield and stability. In vivo study showed higher uptake in PSMA (+) 22Rv1 cells than PSMA (−) PC-3 cells (5.59 ± 0.36 and 1.97 ± 0.22 IA%/10^6 cells at 1 h). It accumulated in 22Rv1 tumor with increasing radioactivity uptake and T/N ratios from 1 to 24 h post-injection. In patients with suspected prostate cancer, SUVmax and T/N ratios increased within 24 h post-injection. Compared with image at 1 h post-injection, more tumor lesions were detected at 6 h and 24 h post-injection. The human organ radiation dosimetry showed gallbladder wall was most critical, liver and kidneys were followed, and the whole-body effective dose was 0.0292 mSv/MBq. Two fine needle aspirates obtained by PET-ultrasound-guided targeted biopsy showed high radioactive signal by autoradiography, with 100% PSMA expression in cytoplasm and 30% expression in nucleus.

Conclusion ^{64}Cu-PSMA-BCH was PSMA specific and showed high stability in vivo with lower uptake in liver than ^{64}Cu-PSMA-617. Biodistribution in mice and PCa patients showed similar profile compared with other PSMA ligands and it was safe with moderate effective dosimetry. The increased tumor uptake and T/N ratios by delayed imaging may facilitate the detection of small lesions and guiding targeted biopsies.

Keywords ^{64}Cu-PSMA · Prostate cancer · PET/CT · Delayed imaging · Targeted biopsies

Introduction

Prostate cancer (PCa) is common among men. PSMA PET/CT has shown high sensitivity and specificity in identifying sites of PCa, and some studies have demonstrated that PSMA-based PET/CT and PET/MR can give accurate location of tumor lesions in primary PCa superior to MRI [1, 2], which offers the possibility that PSMA PET images prior to biopsy giving a simpler criteria for targeted biopsy. Our group had tried ^{68}Ga-PSMA PET-ultrasound fusion targeted biopsies, which improved the detection rate of PCa and decrease the possibility of repeated biopsy [3]. Unfortunately, limited by the short half-life of ^{68}Ga, the images were obtained at 1 h post-injection (p.i.) with high radioactivity

Teli Liu, Chen Liu and Zhongyi Zhang contributed equally to this work.

This article is part of the Topical Collection on Radiopharmacy

✉ Steven P. Rowe
srowe8@jhmi.edu

✉ Hua Zhu
zhuhuananjing@163.com

✉ Zhi Yang
pekyz@163.com

Extended author information available on the last page of the article

in bladder, which lead the low contrast between the PCa and background.

Radiopharmaceuticals labeled with radionuclides having longer half-life can be used in delayed imaging, potentially leading to higher tumor-to-background contrast. Because of the internalization of PSMA radiotracers, the contrast in tumor lesions increases at longer time points after injection, with the radioactivity in non-target organs significantly decreasing at later time points. Among such radionuclides, copper-64 (^{64}Cu) was deemed to be a good choice due to its moderate half-life (12.7 h) and high resolution [4].

^{64}Cu labeled PSMA-targeting probes, ^{64}Cu-PSMA-617 [5–9], ^{64}Cu-DOTA-scFv-anti-PSMA [10], and ^{64}Cu-CA003 [11] have been reported. ^{64}Cu-PSMA-617 showed high diagnostic accuracy for primary LN staging [5, 6]. But the preclinical and in-man studies of ^{64}Cu-PSMA-617 demonstrated high uptake in liver and the in vivo stability showed most of ^{64}Cu-PSMA-617 had been dissociated within 2 h [7–9]. This was possibly due to endogenous proteins involved in copper metabolism transchelating ^{64}Cu from DOTA [12–14]. As human copper transporter 1 is expressed in most tumors, $^{64}CuCl_2$ itself can be used for the diagnosis of PCa [15]. The dissociation of ^{64}Cu from ^{64}Cu-PSMA-617 in vivo not only may lead extra radiation exposure of liver but also could affect the detection of some liver metastases. Compared with DOTA, triaza macrocyclic compounds, such as NOTA and its derivatives, have been reported to chelate ^{64}Cu with higher in vivo stability [16, 17]. In order to obtain high quality images for PCa imaging and give delayed images for improved detection of sites of disease, we prepared a ^{64}Cu labeled radiotracer, ^{64}Cu-PSMA-BCH, with a NOTA-conjugated precursor. The in vitro and in vivo studies were performed to evaluate the stability, PSMA specificity, radiation safety, and tumor targeting of ^{64}Cu-PSMA-BCH.

Materials and experiments

General

$^{64}CuCl_2$ was obtained from the department of Nuclear Medicine, Peking University of Cancer Hospital. All chemicals, reagents and solvents were purchased commercially without further purification. Sep-Pak C18-Light cartridges were purchased from Waters. The product was analyzed by reversed-phase high performance liquid chromatography (RP-HPLC; Eclipse Plus C18, 4.5 × 250 mm, 5 μm; Agilent) performed using a linear A-B gradient (15–60% of B in 15 min) with a flow of 1 mL/min. Solvents were 0.1% aqueous TFA (A) and 0.1% TFA in acetonitrile (B). The HPLC system was equipped with UV and γ detectors. UV absorbance was measured at 220 nm. Micro-PET was performed on Super Argus PET (Sedecal, Spain). PET/CT scans were obtained on a Biograph mCT Flow 64 scanner (Siemens, Erlangen, Germany) with unenhanced low-dose CT. PSMA (+) 22Rv1 and PSMA (−) PC-3 cell lines were obtained from China Cell Line Resource.

Cell culture and animal models

Human prostate cancer cell lines 22Rv1 and PC-3 were cultured and the tumor models were established as previously reported [18]. All animal experiments were conducted in accordance with the guidelines approved by Peking University Cancer Hospital Animal Care and Use Committee.

Radiochemistry and quality control

$^{64}CuCl_2$ was obtained in solution of 0.01 M HCl (3.7 GBq/mL) [4]; 5 μL of PSMA-BCH (2 mM), 200 μL of NaAc (0.1 M), and 50 μL of $^{64}CuCl_2$ (187 MBq) were added in a tube and reacted at 95 °C for 10 min. After cooling to room temperature, ^{64}Cu-PSMA-BCH was purified by C18 Light Cartridge and obtained as shown in supporting information. ^{64}Cu-PSMA-BCH was diluted with saline for further studies, analyzed by radio-HPLC for radiochemical purity, and tested for pH value and sterility.

The detail of partition coefficient, in vitro stability, and pharmacokinetics in blood was provided in supplemental materials.

In vitro cell uptake assay

PSMA (+) 22Rv1 and PSMA (−) PC-3 cell lines were used and the cell uptake study was performed as shown in supporting information. For blocking, 0.5 μg of ZJ-43 ((S)-2-(3-((S)-1-carboxy-3-methylbutyl)ureido), pentanedioic acid), a PSMA inhibitor, was added.

Biodistribution

Biodistribution of ^{64}Cu-PSMA-BCH in normal BALB/c male mice was performed (see supporting information), and the results were expressed as the percent of injected dose per gram (ID%/g).

Micro-PET imaging, biopsy, and histology study in tumor model mouse

A total of 18.7 MBq of ^{64}Cu-PSMA-BCH were injected into mice bearing 22Rv1 and PC-3 vial a tail vein. At 3, 12, and 20 h p.i., the mice were anaesthetized and performed micro-PET imaging on Super Argus PET (Sedecal, Spain) acquired with 80 mm diameter Transaxial FOV, OSEM 3D reconstruction algorithms with attenuation, and random corrections. Finally, the images were displayed by MMWKS Super Argus. The milicounts/sec values of ROI (regions of interest) over tumor, kidneys and liver were collected.

Radioautography and immunohistochemistry

The samples were stored on slides with 10% neutral formaldehyde fixative and exposed on a phosphorus plate (Perkin-Elmer, USA) for 12 h. The plate was scanned using a phosphor imaging system (Cyclone, Packard) to obtain the images. The slides were prepared and analyzed for PSMA expression by immunochemistry as described previously [7].

PET/CT imaging and analysis

With the approval of Ethics Committee of Beijing Cancer Hospital (No. 2017KT97), four patients (age 77.25 ± 5.36, range 68–81, PSA 35.40 ± 31.05 ng/mL, range 8.5–86.15; Gleason score 8.25 ± 0.43, range 8–9) who were highly suspected with prostate cancer and were clinically appropriate for biopsies were included in this study. Among them, only one patient had performed operation. The detail information of four patients were shown in Table 1. Three patients without metastasis were performed whole-body PET/CT scans at 1 and 24 h p.i. and pelvic cavity scans at 6 h p.i. One patient with multiple bone and lymph nodes metastases performed whole-body PET/CT scans at 1, 6, and 24 h p.i. Imaging was performed and all images were read by 2 experienced nuclear medicine specialists; the SUVmean, radioactivity concentration (Bq/mm^3) and volume (mm^3) of each organ, and SUVmax of tumor lesions were obtained as literature as previously reported [18].

Absorbed dosimetry

The radioactivity concentration (Bq/mm^3) and volume (mm^3) were used for calculating ID% of each organ. And the data was used for estimating human organ radiation dosimetry. OLINDA/EXM 2.0 software (Hermes Medical Solution, Sweden) was used with adult male model without special kinetics.

PET-ultrasound-guided targeted biopsy

After imaging at 24 h p.i., the images were reconstructed and analyzed, then the patients were performed classic ultrasound-guided biopsies with visual fusion of PET images according to PROMISE criteria (version 1.0) as reported [3, 19]. The samples were stored in 10% neutral formaldehyde fixative and exposed on a phosphorus plate (Perkin-Elmer, USA) for 12 h. The plate was scanned using a phosphor imaging system (Cyclone, Packard) to obtain the images. The preparation of slides, hematoxylin-eosin staining and immunochemistry for PSMA was performed as described previously [7].

Results

Radiochemistry and quality control

^{64}Cu-PSMA-BCH was prepared with the yield over 95% and the radiochemical purity over 99% analyzed by radio-HPLC. The retention time of ^{64}Cu-PSMA-BCH and $^{64}Cu^{2+}$ were 9.34 min and 3.46 min, respectively. The specific activity of ^{64}Cu-PSMA-BCH was 14.3 ± 1.91 GBq/μmol. After diluted with saline, the quality control of ^{64}Cu-PSMA-BCH was performed, and the result was shown in Table S1.

Partition coefficient and in vitro stability

The log P value of ^{64}Cu-PSMA-BCH was calculated as −2.46 ± 0.11, indicating ^{64}Cu-PSMA-BCH was hydrophilic.

After incubation in saline and 5% human serum albumin (HSA) at 37 °C for 36 h, the radiochemical purity of ^{64}Cu-PSMA-BCH was over 95% (Fig. S3), indicating ^{64}Cu-PSMA-BCH was stable in vitro.

Cell uptake and binding affinity

The uptake of ^{64}Cu-PSMA-BCH in 22Rv1 cells increased with time between 5 and 120 min; the highest values were 5.71 ± 0.16%IA/10^6 cells at 120 min (Fig. 1a). The uptake in 22Rv1 decreased to 3.44 ± 0.13%IA/10^6 ($P < 0.001$) when co-incubated with excess ZJ-43. While the highest uptake in PC-3 was 1.79 ± 0.20%IA/10^6 cells at 60 min and the uptake could not be blocked by ZJ-43 (1.86 ± 0.17, $P > 0.05$).

Table 1 Characteristics of patients (n = 4)

No	Age (y)	Weight (kg)	PSA (ng/mL)	Gleason score	Clinical stage	Pathological stage	Injected dose (MBq)
1	68	50	8.5	5 + 4	T2 N0 M0	T2	119
2	81	75	86.15	4 + 4	T3b N0M0	NA	152
3	80	60	35.16	4 + 4	T3a N0 M0	NA	165
4	80	71	11.80	4 + 4	T4 N1 M1	NA	160.76

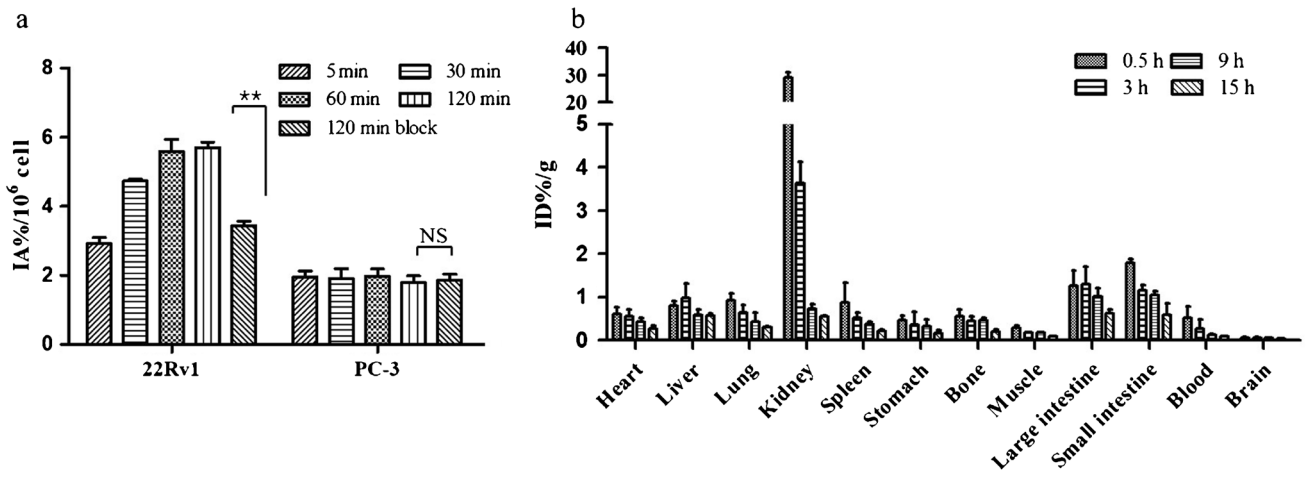

Fig. 1 **a** In vitro cell uptake of ^{64}Cu-PSMA-BCH in 22Rv1 and PC-3 cell lines, blocking with 1 μg/well of ZJ-43; **b** biodistribution of ^{64}Cu-PSMA-BCH in healthy BALB/c male mice. **: $P < 0.001$; NS: $P > 0.05$

Pharmacokinetics

The in vivo metabolism of ^{64}Cu-PSMA-BCH in blood pool was determined by a two-compartmental model using GraphPad prism 5.0 (Fig. S3). The equation for ^{64}Cu-PSMA-BCH in BALB/c mice was $Ct = 0.3315 + 20.60 * \exp(-3.333t) + 9.73 * \exp(-0.0649t)$, with the half-life of 10.68 min for the distribution phase and the half-life of 0.208 min for the elimination phase, respectively.

Biodistribution

In normal BALB/c male mice, kidney showed the highest accumulation of ^{64}Cu-PSMA-BCH (Fig. 1b, Table S2); the values were 29.15 ± 1.85 ID%/g at 0.5 h p.i. and 0.54 ± 0.12 ID%/g at 15 h p.i. ^{64}Cu-PSMA-BCH cleared out from blood with the uptake of 0.52 ± 0.26%ID/g to 0.08 ± 0.01 ID%/g from 0.5 to 15 h p.i.. The uptake in liver decreased form 0.80 ± 0.11 to 0.56 ± 0.07 ID%/g from 0.5 to 15 h p.i., which was much lower than that of ^{68} Ga-PSMA-617 (the uptake in liver was reported as 12.65 ± 0.75 to 9.08 ± 0.57 ID%/g from 0.5 to 12 h p.i. in ICR mice and from 24.10 ± 2.34 to 8.13 ± 1.08 ID%/g from 4 to 24 h p.i. in BALB/c mice) [5, 7].

Micro-PET imaging

Micro-PET imaging was performed on a male BALB/c nude mouse bearing 22Rv1 and PC-3 tumors. 22Rv1 tumor, kidneys, bladder, and liver were clearly visualized, while the PC-3 tumors cannot be observed (Fig. 2a). The radioactivity accumulation in liver and 22Rv1 tumor was lightly increased

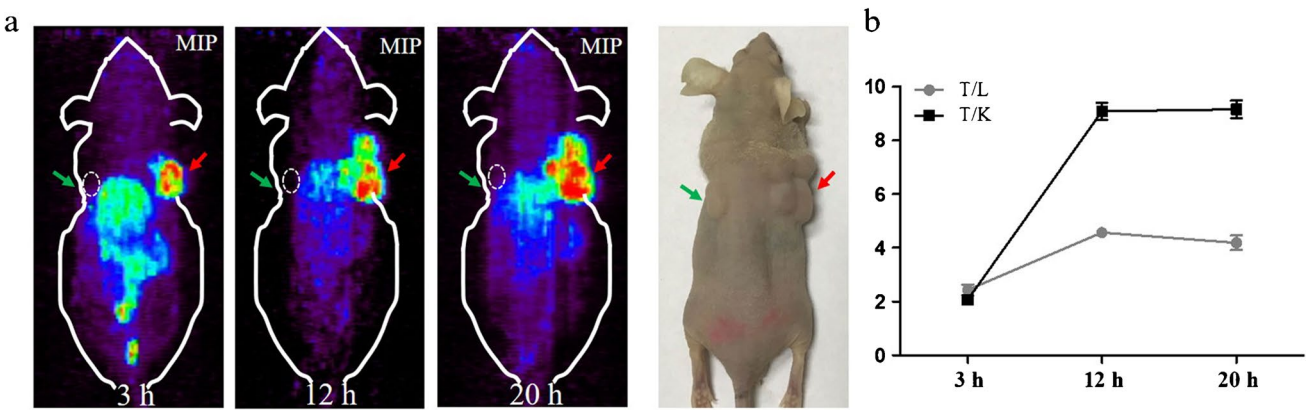

Fig. 2 **a** Micro-PET MIP images of ^{64}Cu-PSMA-BCH in mice bearing 22Rv1 and PC-3 xenograft tumors at 3 h, 12 h, and 20 h p.i., green arrows and white circles indicate PC-3 tumors, red arrows indicate 22Rv1 tumors; **b** T/N ratios of ^{64}Cu-PSMA-BCH in mice bearing 22Rv1 and PC-3 at 3 h, 12 h, and 20 h p.i., T/L, 22Rv1 tumor-to-liver ratio; T/K, 22Rv1 tumor-to-kidney ratio

within 20 h, while the uptake in kidney was decreased and the kidneys were nearly invisible at 12 h and 20 h p.i. At 12 h p.i., only 22Rv1 tumor and liver were observed. The counts of ROIs over kidneys, liver, 22Rv1, and PC-3 tumors were measured. The 22Rv1/PC-3 tumors and 22Rv1/kidney ratios were increased with time (from 3.92 to 20.30 and from 0.2 to 2.99, respectively) between 3 and 12 h p.i. (Fig. S2b). Compared with reported data of ^{68} Ga-PSMA-617, the radioactivity of ^{64}Cu-PSMA-BCH in liver is lower, which was coincidence with the biodistribution result in normal BALB/c mice.

PET/CT imaging

Four patients who were highly suspected with PCa were included in this study and conducted ^{64}Cu-PSMA-BCH PET/CT imaging. Among four patients, only one had performed operation. At 1 h post-injection, bladder, kidneys, lacrimal glands, parotid glands, submandibular glands, liver, proximal small bowel, and tumor lesion were clearly observed, which was coincidence with other PSMA radioligands (Fig. 3a, Table S3). The uptake in liver was increased and the SUVmean was increased from 4.38 to 5.31 between 1 and 24 h p.i. Though kidneys, lacrimal glands, parotid glands, and submandibular glands were visible at 24 h p.i., the SUVmean values were decreased. The SUVmax of tumor lesions in three PCa patients without metastases were increased between 1 and 24 h p.i. (Fig. 3b), while those of bladder and other organs was decreased. The tumor-to-bladder and tumor-to-background contrast increased (Figure S4).

In this study, one PCa patient with multiple metastases was included. At 6 and 24 h p.i., more tumor lesions were observed and the SUVmax values were higher than those at 1 h p.i.; the highest values occurred at 6 h p.i. (Figs. 4 and S5–S7).

Radiation dosimetry estimates

With the biodistribution data of ^{64}Cu-PSMA-BCH patients with primary prostate cancer, the human organ radiation dosimetry of ^{64}Cu-PSMA-BCH was calculated using OLINDA/EXM 2.0 software package. The estimated dosimetry was shown in Table 2. Gallbladder wall was the most critical organ (2.04E + 00 mGy/MBq), followed by liver (1.45E-02 mGy/MBq) and kidneys (9.47E-03 mGy/MBq). The effective dose was 0.0292 mSv/MBq, which means the effective dose of a patient was 4.3 mSv when injected with 4 mCi of ^{64}Cu-PSMA-BCH. The whole-body effective dose of ^{18}F-FDG that International Commission on Radiological Protection's (ICRP) is 0.019 mSv/MBq, equating to an effective dose for a 70 kg adult man (4.9 mSv). The effective dose of ^{64}Cu-PSMA-BCH therefore is comparable to ^{18}F-FDG for a male.

PET-ultrasound-guided targeted biopsy and histology

After imaging at 24 h p.i., patients with suspected primary prostate cancer underwent PSMA-targeted PET-ultrasound fusion guided biopsies. Figure 5a showed the ^{64}Cu-PSMA-BCH PET/CT images of one patient (age 80 years, PSA 31.6 ng/mL) at 24 h p.i. First two targeted scores were kept in 10% neutral formaldehyde fixative and exposed to a screen (Fig. 5c). The radioautography images clearly displayed

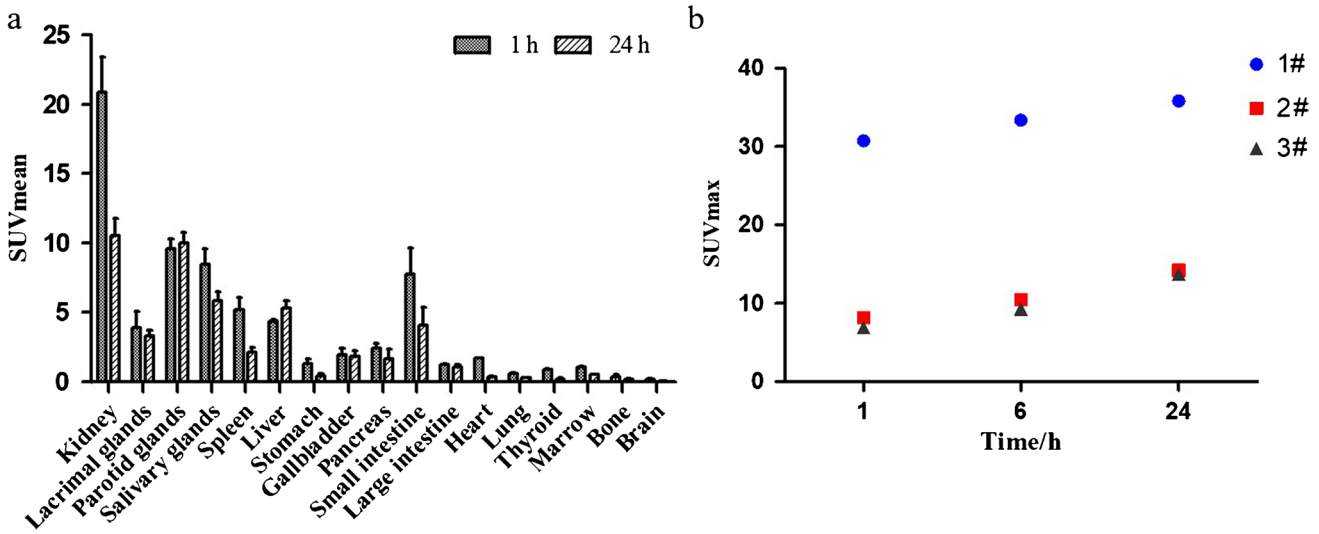

Fig. 3 **a** Organ biodistribution of ^{64}Cu-PSMA-BCH in patients with primary prostate cancer (n = 3); **b** SUVmax values of tumor lesions in three patients with primary prostate cancer, 1#, 2#, and 3# represent three tumor lesions from patient 1, 2, and 3, respectively

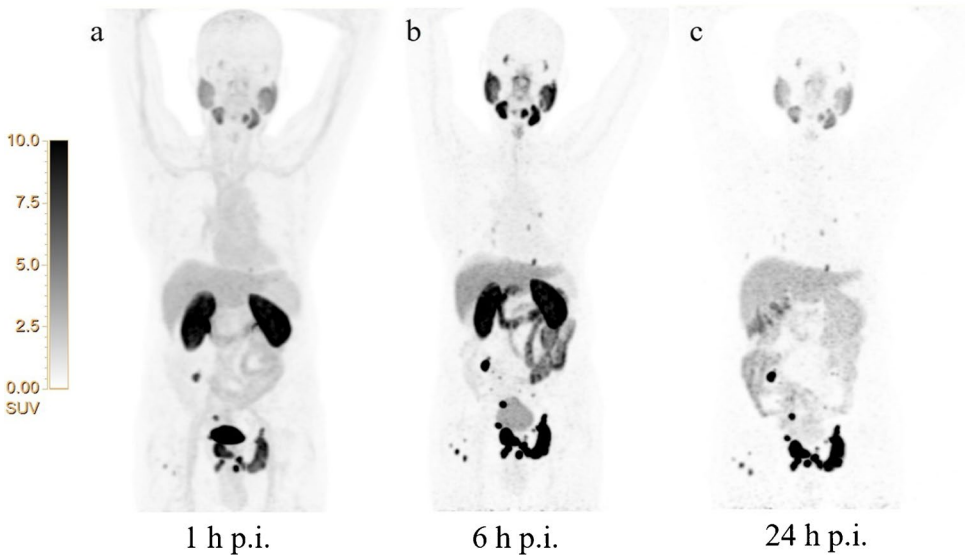

Fig. 4 MIP PET images of ^{64}Cu-PSMA-BCH in an 80-year-old patient (PSA 11.80 ng/mL, GS 4 + 4) at 1 h (**a**), 6 h (**b**), and 24 h (**c**) post-injection

Table 2 Estimated human organ absorbed radiation dosimetry of ^{64}Cu-PSMA-BCH (n = 3)

Organ	Equivalent dose per unit injected dose activity (mGy/MBq)
Adrenals	1.84E-03
Brain	4.62E-04
Esophagus	5.93E-04
Eyes	1.48E-04
Gallbladder wall	2.04E + 00
Left colon	5.84E-04
Small intestine	5.61E-04
Stomach wall	6.74E-04
Right colon	7.09E-04
Rectum	1.39E-04
Heart wall	8.32E-04
Kidneys	9.47E-03
Liver	1.45E-02
Lungs	1.68E-03
Pancreas	7.16E-04
Prostate	1.32E-04
Salivary glands	1.24E-04
Red marrow	4.00E-04
Osteogenic cells	5.20E-03
Spleen	1.40E-03
Testes	6.44E-05
Thymus	3.03E-04
Thyroid	2.08E-04
Urinary bladder wall	9.43E-05
Total body	7.06E-04
Effective dose (mSv/MBq)	0.0292

the morphology of corresponding tissues (Fig. 5d). The HE (hematoxylin–eosin) and PSMA immunohistochemical staining of targeted biopsies showed Gleason score of 4 + 4 with high PSMA expression (100%) in enchylema (Fig. 5e1–f2).

Discussions

PCa is widely concerned as its high incidence. Accurate diagnosis and staging are essential for making treatment planning. PSMA is overexpressed in PCa with high specificity; it has become an important target for the diagnosis and therapy of PCa. Multiple radiotracers targeting PSMA have been developed and PSMA PET/CT showed high sensitivity and specificity for the detection of PCa. In this study, we prepared a tracer labeled with long half-life radionuclide, copper-64. Among the reported ^{64}Cu-PSMA tracers, most of them were DOTA-conjugators. ^{64}Cu-DOTA complexes was considered with relatively low in vivo stability, especially under acidic condition, which may lead to the transchelation of ^{64}Cu ion to serum protein [20]. Compared with DOTA, NOTA has higher affinity to copper-64 and the resulting complexes are more stable in vivo [16].

^{64}Cu-PSMA-BCH showed lower radioactivity accumulation in liver, and the uptake of ^{64}Cu-PSMA-BCH in kidneys was higher than other organs, which was different from DOTA-conjugated complexes. Indicating ^{64}Cu-PSMA-BCH was more stable in vivo.

^{64}Cu-PSMA-BCH specifically accumulated in PSMA(+) 22Rv1 cells and tumor, which can be blocked by a PSMA inhibitor [21], while PSMA(−) PC-3 cells or tumor showed low uptake of ^{64}Cu-PSMA-BCH. In human PET images, ^{64}Cu-PSMA-BCH accumulated in kidneys, bladder, submandibular glands, parotid glands, and

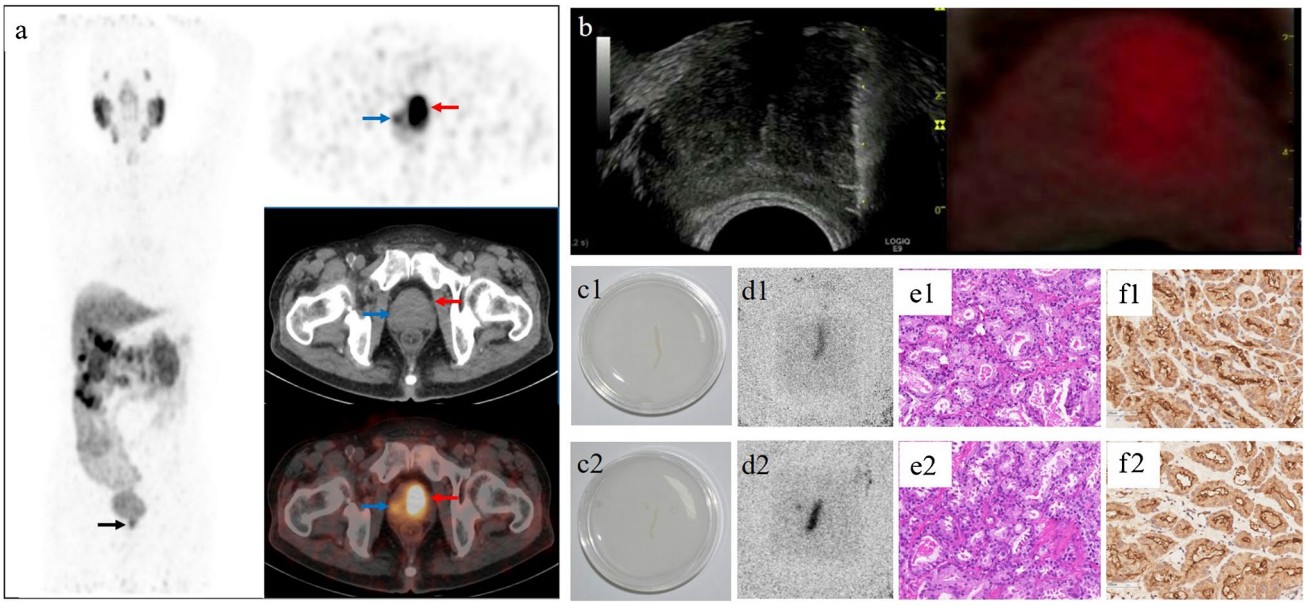

Fig. 5 ^{64}Cu-PSMA-BCH PET-ultrasound fusion guided target biopsy and histological certification. **a** ^{64}Cu-PSMA-BCH PET/CT images of a PCa patient (80-year-old, PSA 35.6 ng/mL) at 24 h p.i.; **b** prostate biopsy with real-time ^{64}Cu-PSMA-BCH PET/ultrasound fusion; **c1**, **c2** pictures of two targeted puncture biopsies in 10% neutral formaldehyde fixative; **d1**, **d2** autoradiograph images of two targeted puncture biopsies; **e1**, **e2** HE staining of two biopsies (×20) with the Gleason score of 4 + 4; **f1**, **f2** PSMA immunohistochemical analysis of two biopsies (×20). 1: The needle from the region of blue arrow; 2: the needle from the region of red arrow

lacrimal glands, which showed classic property of PSMA targeted tracers. The in vitro and in vivo data indicated ^{64}Cu-PSMA-BCH was specific to PSMA.

^{64}Cu-PSMA-BCH increasingly accumulated in primary prostate cancer of three patients without metastases within 24 h; it was fast cleared out from bladder and other organs, which contributed increasing tumor-to-bladder and tumor-to-background contrast and which may be beneficial for guiding biopsies.

Though the long half-life of ^{64}Cu lead to higher effective dose of ^{64}Cu-PSMA-BCH (0.0292 mSv/MBq) than many ^{68}Ga and ^{18}F labeled PSMA radiotracers [18], the long half-life of ^{64}Cu also allowed lower injected dose. The lower injected dose and higher effective dose of ^{64}Cu-PSMA-BCH make comparable radiation dose to patients. ^{64}Cu-PSMA-BCH was not only safe for PET/CT imaging. Long half-life of radionuclide may also allow delayed imaging. Some studies had reported that delayed PSMA PET/CT imaging can increase the uptake in tumor and may detect more tumor lesions with small volume or low PSMA expression [22–24]. In this study, the bone and lymph nodes metastases of one PCa patient with multiple metastases were clearly observed at 6 h p.i., while some of them were invisible at 1 h p.i. The delayed imaging may detect more tumor lesions, especially for the tumor lesions with low SUVmax and tumor-to-background ratio at 1 h p.i. The detection of some distant metastases may change the treatment strategy.

Not only for detecting tumors, delayed PSMA PET/CT imaging of ^{64}Cu-PSMA-BCH may have more application in clinic. Our group had reported a study that performed PSMA PET/CT prior to biopsy and then PSMA PET-ultrasound fusion targeted biopsies, which improved the detection rate and decrease possibility of repeated biopsies [3]. As shown in Figure S4, the tumor lesion at the right upper lobe of prostate was invisible at 1 h p.i., but it was clearly observed at the pelvic images at 6 h p.i. and images at 24 h p.i. The increased uptake of tumors and contrasts of ^{64}Cu-PSMA-BCH in delayed images are benefit for offering more accurate sites of PSMA PET images-ultrasound fused targeted biopsies. The preliminary study of ^{64}Cu-PSMA-BCH PET-ultrasound fused targeted biopsies in this study demonstrated the effectiveness of delayed imaging for locating the puncture sites. With the limited number of volunteers, more studies are needed to fully verify the potential of delayed ^{64}Cu-PSMA-BCH PET imaging for targeted biopsies.

Recently, PSMA radioligand therapy (PRLT) showed inspiring therapeutic results for patients with metastatic castration resistant prostate cancer (mCRPC) [25]. ^{64}Cu-PSMA-BCH delayed PET/CT imaging provides an approach for multi-temporal monitoring the uptake of radiotracers in tumors, especially for later time point which is beyond ^{68} Ga and ^{18}F labeled radiotracers can detect. Thus, to assess the potential benefits for patients from PRLT and then screen the appropriate candidates for PRLT may be another application of ^{64}Cu-PSMA-BCH in clinic.

There are many mature PSMA radiotracers which are widely applicated for PCa PET imaging, most of them are radiolabeled with Galium-68 and Fluorine-18. Compared with them, ^{64}Cu-PSMA-BCH was suitable for delayed imaging and guiding biopsies as the longer half-life, good in vivo stability, high tumor uptake, and retention. But because of the accessibility and high cost of copper-64, ^{64}Cu-PSMA-BCH was unsuitable for only diagnosis of PCa; more application of ^{64}Cu-PSMA-BCH in clinical should be explored in our ongoing study.

Conclusion

In this study, ^{64}Cu-PSMA-BCH was demonstrated with higher in vivo stability than DOTA-conjugated complexes. ^{64}Cu-PSMA-BCH was PSMA specific and can be used for PSMA PETT/CT imaging of PCa patients. As the longer half-life of ^{64}Cu and the internalization of radiotracers, delayed imaging with ^{64}Cu-PSMA-BCH was meaningful in detecting small or insidious lesions, guiding accurate targeted biopsies and screening appropriate mCRPC patients for PRLT. But limited with the number of included volunteers, more studies are needed to further verify the value of the clinical applications of ^{64}Cu-PSMA-BCH.

Supplementary Information The online version contains supplementary material available at https://doi.org/10.1007/s00259-021-05426-9.

Funding This study was fund by Beijing Natural Science Foundation (Nos. 7194246, 7202028), Science Foundation of Peking University Cancer Hospital 2020–17, Beijing Excellent Talents Funding (2017000021223ZK33), Beijing Millions of Talents Projects A level funding (No. 2019A38), and Municipal Administration of Hospitals-Yangfan Project (ZYLX201816).

Declarations

Ethical approval All animal experiments were conducted in accordance with the guidelines approved by Peking University Cancer Hospital Animal Care and Use Committee. All procedures performed in studies involving human participants were in accordance with the ethical standards of the institutional and/or national research committee and with the 1964 Helsinki declaration and its later amendments or comparable ethical standards. The study was approved by Ethics Committee of Beijing Cancer Hospital and Institute (No.2017KT97).

Consent to participate Informed consent was obtained from all individual participants included in the study.

Conflict of interest The authors declare no competing interests.

References

1. Perera M, Papa N, Christidis D, Wetherell D, Hofman MS, Murphy DG, et al. Sensitivity, specificity, and predictors of positive ^{68}Ga-prostate-specific membrane antigen positron emission tomography in advanced prostate cancer: a systematic review and meta-analysis. Eur Urol. 2016;70(6):926–37. https://doi.org/10.1016/j.eururo.2016.06.021.
2. Fendler WP, Schmidt DF, Wenter V, Thierfelder KM, Zach C, Stief C, et al. ^{68}Ga-PSMA PET/CT detects the location and extent of primary prostate cancer. J Nucl Med. 2016;57(11):1720–5. https://doi.org/10.2967/jnumed.116.172627.
3. Liu C, Liu T, Zhang Z, Zhang N, Du P, Yang Y, et al. PSMA PET/CT and standard plus PET/CT-ultrasound fusion targeted prostate biopsy can diagnose clinically significant prostate cancer in men with previous negative biopsies. J Nucl Med. 2020;61(9):1314–9. https://doi.org/10.2967/jnumed.119.235333.
4. Xie Q, Zhu H, Wang F, Meng X, Ren Q, Xia C, et al. Establishing reliable Cu-64 production process: from target plating to molecular specific tumor micro-PET imaging. Molecules. 2017;22(4):641–50. https://doi.org/10.3390/molecules22040641.
5. Cui C, Hanyu M, Hatori A, Zhang Y, Xie L, Ohya T, et al. Synthesis and evaluation of [^{64}Cu]PSMA-617 targeted for prostate-specific membrane antigen in prostate cancer. Am J Nucl Med Mol Imaging. 2017;7(2):40–52.
6. Cantiello F, Gangemi V, Cascini GL, Calabria F, Moschini M, Ferro M, et al. Diagnostic accuracy of ^{64}copper prostate-specific membrane antigen positron emission tomography/computed tomography for primary lymph node staging of intermediate-to high-risk prostate cancer: our preliminary experience. Urology. 2017;106:139–45. https://doi.org/10.1016/j.urology.2017.04.019.
7. Han XD, Liu C, Liu F, Xie QH, Liu TL, Guo XY, et al. ^{64}Cu-PSMA-617: a novel PSMA-targeted radio-tracer for PET imaging in gastric adenocarcinoma xenografted mice model. Oncotarget. 2017;8(43):74159–69. https://doi.org/10.18632/oncotarget.18276.
8. Grubmüller B, Baum RP, Capasso E, Singh A, Ahmadi Y, Knoll P, et al. ^{64}Cu-PSMA-617 PET/CT imaging of prostate adenocarcinoma: first in-human studies. Cancer Biother Radiopharm. 2016;31(8):277–86.
9. Hoberuck S, Wunderlich G, Michler E, Holscher T, Walther M, Seppelt D, et al. Dual-time-point ^{64}Cu-PSMA-617-PET/CT in patients suffering from prostate cancer. J Labelled Comp Radiopharm. 2019;62(8):523–32. https://doi.org/10.1002/jlcr.3745.
10. Wong P, Lin L, Chea J, Delgado MK, Crow D, Poku E, et al. PET imaging of ^{64}Cu-DOTA-scFv-anti-PSMA lipid nanoparticles (LNPs): enhanced tumor targeting over anti-PSMA scFv or untargeted LNPs. Nucl Med Biol. 2017;47:62–8. https://doi.org/10.1016/j.nucmedbio.2017.01.004.
11. Dos Santos JC, Beijer B, Bauder-Wust U, Schafer M, Leotta K, Eder M, et al. Development of novel PSMA ligands for imaging and therapy with copper isotopes. J Nucl Med. 2019. https://doi.org/10.2967/jnumed.119.229054.
12. Boswell CA, Sun X, Niu W, Weisman GR, Wong EH, Rheingold AL, et al. Comparative in vivo stability of copper-64-labeled cross-bridged and conventional tetraazamacrocyclic complexes. J Med Chem. 2004;47(6):1465–74.
13. Bass LA, Wang M, Welch MJ, Anderson CJ. In vivo transchelation of copper-64 from TETA-octreotide to superoxide dismutase in rat liver. Bioconjug Chem. 2000;11(4):527–32.
14. Woodin KS, Heroux KJ, Boswell CA, Wong EH, Weisman GR, Niu W, et al. Kinetic inertness and electrochemical behavior of copper(II) tetraazamacrocyclic complexes: possible implications for in vivo stability. Eur J Inorg Chem. 2005;2005(23):4829–33. https://doi.org/10.1002/ejic.200500579.
15. Ceci F, Fendler W, Eiber M. A new type of prostate cancer imaging: will $^{64}CuCl_2$ PET/CT flourish or vanish? J Nucl Med. 2018;59(3):442–3. https://doi.org/10.2967/jnumed.117.199885.
16. Wadas TJ, Wong EH, Weisman GR, Anderson CJ. Coordinating radiometals of copper, gallium, indium, yttrium, and

zirconium for PET and SPECT imaging of disease. Chem Rev. 2010;110(5):2858–902.
17. Ghosh SC, Pinkston KL, Robinson H, Harvey BR, Wilganowski N, Gore K, et al. Comparison of DOTA and NODAGA as chelators for ^{64}Cu-labeled immunoconjugates. Nucl Med Biol. 2015;42(2):177–83. https://doi.org/10.1016/j.nucmedbio.2014.09.009.
18. Liu T, Liu C, Xu X, Liu F, Guo X, Li N, et al. Preclinical evaluation and pilot clinical study of Al^{18}F-PSMA-BCH for prostate cancer imaging. J Nucl Med. 2019;60:1284–92. https://doi.org/10.2967/jnumed.118.221671.
19. Eiber M, Herrmann K, Calais J, Hadaschik B, Giesel FL, Hartenbach M, et al. Prostate cancer molecular imaging standardized evaluation (PROMISE): proposed miTNM classification for the interpretation of PSMA-ligand PET/CT. J Nucl Med. 2018;59(3):469–78. https://doi.org/10.2967/jnumed.117.198119.
20. Qin C, Liu H, Chen K, Hu X, Ma X, Lan X, et al. Theranostics of malignant melanoma with $^{64}CuCl_2$. J Nucl Med. 2014;55(5):812–7. https://doi.org/10.2967/jnumed.113.133850.
21. Olszewski RT, Bukhari N, Zhou J, Kozikowski AP, Wroblewski JT, Shamimi-Noori S, et al. NAAG peptidase inhibition reduces locomotor activity and some stereotypes in the PCP model of schizophrenia via group II mGluR. J Neurochem. 2004;89(4):876–85. https://doi.org/10.1111/j.1471-4159.2004.02358.x.
22 Kunikowska J, Kujda S. ^{68}Ga-PSMA PET/CT in recurrence prostate cancer. Should we perform delayed image in cases of negative 60 minutes postinjection examination? Clin Nucl Med. 2020;45(4):e213–4. https://doi.org/10.1097/rlu.0000000000002966.
23. Derlin T, Weiberg D, von Klot C, Wester H-J, Henkenberens C, Ross TL, et al. ^{68}Ga-PSMA I&T PET/CT for assessment of prostate cancer: evaluation of image quality after forced diuresis and delayed imaging. Eur Radiol. 2016;26(12):4345–53. https://doi.org/10.1007/s00330-016-4308-4.
24. Schmuck S, Nordlohne S, von Klot C-A, Henkenberens C, Sohns JM, Christiansen H, et al. Comparison of standard and delayed imaging to improve the detection rate of [^{68}Ga]PSMA I&T PET/CT in patients with biochemical recurrence or prostate-specific antigen persistence after primary therapy for prostate cancer. Eur J Nucl Med Mol Imaging. 2017;44(6):960–8. https://doi.org/10.1007/s00259-017-3669-5.
25. Barber TW, Singh A, Kulkarni HR, Niepsch K, Billah B, Baum RP. Clinical outcomes of ^{177}Lu-PSMA radioligand therapy in earlier and later phases of metastatic castration-resistant prostate cancer grouped by previous taxane chemotherapy. J Nucl Med. 2019;60(7):955–62. https://doi.org/10.2967/jnumed.118.216820.

Authors and Affiliations

Teli Liu[1] · Chen Liu[1] · Zhongyi Zhang[2] · Ning Zhang[3] · Xiaoyi Guo[1] · Lei Xia[1] · Jinquan Jiang[1] · Qing Xie[1] · Kun Yan[2] · Steven P. Rowe[4] · Hua Zhu[1] · Zhi Yang[1]

1 Key Laboratory of Carcinogenesis and Translational Research, Ministry of Education/Beijing), NMPA Key Laboratory for Research and Evaluation of Radiopharmaceuticals (National Medical Products Administration), Department of Nuclear Medicine, Peking University Cancer Hospital & Institute, No. 52 Fu-Cheng Rd, Beijing 100142, China

2 Key Laboratory of Carcinogenesis and Translational Research (Ministry of Education/Beijing), Department of Ultrasonography, Peking University Cancer Hospital & Institute, No. 52 Fu-Cheng Rd, Beijing 100142, China

3 Key Laboratory of Carcinogenesis and Translational Research (Ministry of Education/Beijing), Department of Urology, Peking University Cancer Hospital & Institute, No. 52 Fu-Cheng Rd, Beijing 100142, China

4 The James Buchanan Brady Urology Institute and Department of Urology, and The Russell H. Morgan, Department of Radiology and Radiological Science, Johns Hopkins University School of Medicine, 601 N. Caroline St., Rm. 3233, Baltimore, MD 21287, USA